

Supporting Information

Modifying the Mie resonances and carrier dynamics of silicon nanoparticles by injecting dense electron-hole plasma

Jin Xiang,¹ Jingdong Chen,² Qiaofeng Dai,¹ Shaolong Tie,³ Sheng Lan^{1*}, and Andrey E. Miroshnichenko^{4*}

¹*Guangdong Provincial Key Laboratory of Nanophotonic Functional Materials and Devices, School of Information and Optoelectronic Science and Engineering, South China Normal University, Guangzhou 510006, China*

²*College of Physics and Information Engineering, Minnan Normal University, Zhangzhou 363000, China*

³*School of Chemistry and Environment, South China Normal University, Guangzhou 510006, China*

⁴*School of Engineering and Information Technology, University of New South Wales, Canberra, ACT, 2600, Australia*

*Corresponding Author: slan@scnu.edu.cn and andrey.miroshnichenko@unsw.edu.au

Table of contents

1. Characterization of Si nanoparticles.....	1
2. Dependence of the dielectric constant of Si on the carrier density.....	1
3. Internal mode volume of Si nanospheres.....	2
4. Enhancement factors of the electric field.....	3
5. Luminescence decay of Si nanospheres.....	4
6. Temperature rise in Si nanospheres induced by fs laser pulses.....	4
7. Blue spectral shift, enhancement factor and quantum efficiency.....	5

S1: Characterization of the Si nanoparticles

The Si nanoparticles fabricated by using femtosecond laser ablation were characterized by both scanning electron microscopy (SEM) and transmission electron microscopy (TEM). In Fig. S1(a), we show the energy dispersive spectroscopy (EDS) spectrum measured for a Si nanosphere placed on a quartz (SiO_2) substrate. It is noticed that the spectrum is dominated by Si and O elements (> 99%). The other elements (<1%) come from the quartz (SiO_2) substrate. The crystalline phase of Si nanoparticles was examined by high-resolution TEM, as shown in Fig. S1(b). Each Si nanoparticle is composed of a single crystalline core and an amorphous shell with a thickness of ~ 2 nm.

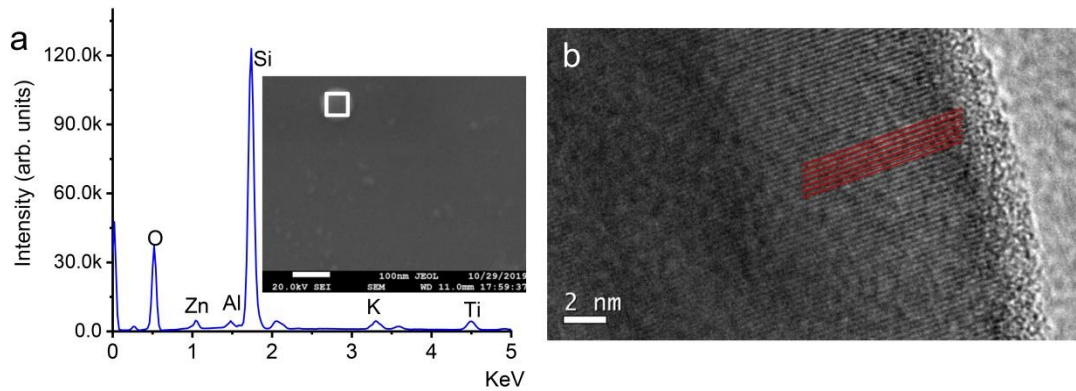


Figure S1: (a) EDS obtained on an area of $0.4 \times 0.4 \mu\text{m}^2$ located at the center of a Si nanosphere (see the inset). (b) TEM image of a typical Si nanosphere. The crystalline phase of the Si nanosphere is indicated by paralleled red lines. The length of the scale bar is 2 nm.

S2: Dependence of the dielectric constant of Si on the carrier density

Based on Eq. (1), one can calculate the dependence of the dielectric constant of Si on the injected carrier density, as shown in Fig. S2. It can be seen that the electron-hole plasma modifies only the real part of the dielectric constant and it has negligible influence on the imaginary part. In the calculation, the variation of the damping time (τ) with the carrier density, which is shown in the inset of Fig. S2(a), has been taken into account.

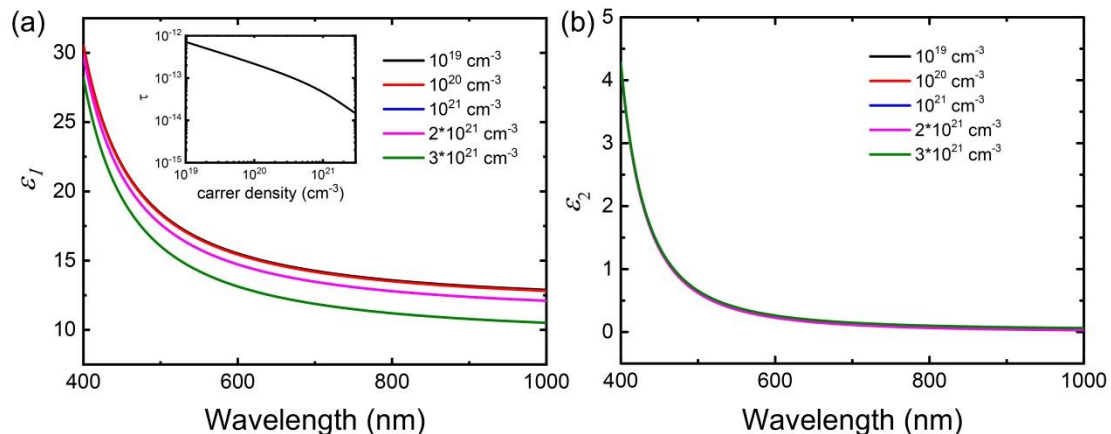


Figure S2: Dependence of the dielectric constant of Si on the injected carrier density. (a) Real part. (b) Imaginary part.

S3: Internal mode volume of Si nanospheres

The sensitivities of the Mie resonances of a Si nanoparticle to the dielectric constant change can be characterized by using the internal mode volume of the Si nanoparticle which is defined as follows^[1]:

$$V_{\text{mode}} = \frac{\int \epsilon E^2 dV}{\max(\epsilon E^2)}. \quad (1)$$

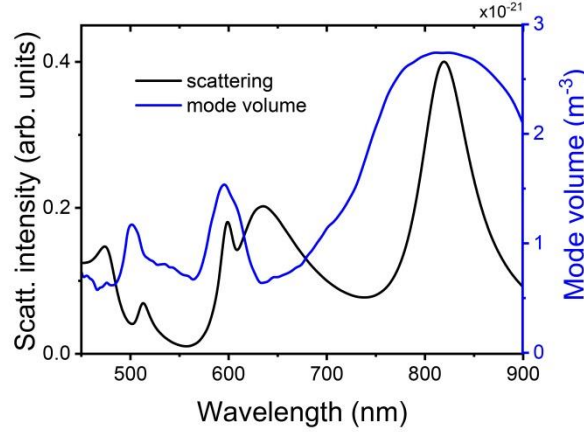


Figure S3: Internal mode volume calculated for the Mie resonances of a Si nanosphere with $d = 200$ nm. The scattering spectrum of the Si nanosphere is also provided for reference.

In Fig. S3, we present the wavelength dependence of the internal mode volume calculated for a Si nanosphere with $d = 200$ nm. It is noticed that the maxima of the internal mode volume appears at the MD resonance of the Si nanosphere. In addition, the internal mode volumes at the MQ and EQ resonances are much larger than that at the ED resonance because the electric field is strongly localized in the Si nanosphere. Therefore, the largest blueshift is expected to occur at the MD resonance, as demonstrated in this work.

S4: Enhancement factors of the electric field

As discussed in the main text, the integrations of $|E|^2$, $|E|^4$ and $|E|^6$ over the volume of a Si nanoparticle can be employed to characterize the single-, two- and three-photon-induced absorption in the Si nanoparticle. In addition, it is also shown that the emission efficiency of the Si nanoparticle can also be characterized by using the integration of $|E|^2$ over the volume

of the Si nanoparticle. In Fig. S4, we show the spectra of $[\int |E(\lambda)|^2 dV]/V$, $[\int |E(\lambda)|^4 dV]/V$, and $[\int |E(\lambda)|^6 dV]/V$ calculated for a Si nanosphere with $d = 200$ nm.

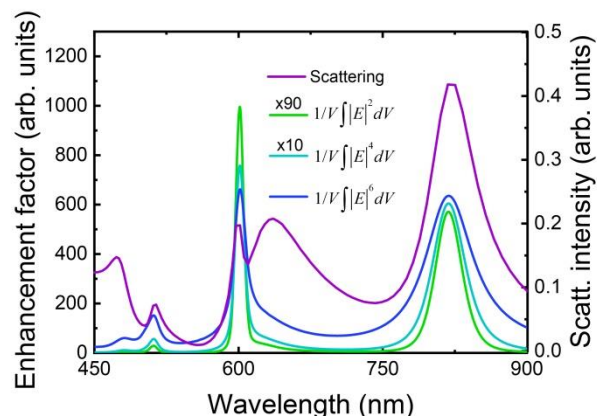


Figure S4: Spectra of $[\int |E(\lambda)|^2 dV]/V$, $[\int |E(\lambda)|^4 dV]/V$, and $[\int |E(\lambda)|^6 dV]/V$ calculated for a Si nanosphere with $d = 200$ nm.

S5: Luminescence decay of Si nanospheres

In order to virtualize the maximum blueshift of the MD resonance of a Si nanoparticle, it is required that the lifetime of the hot electron luminescence emitted by the Si nanoparticle should be short enough. In Figure S4, we present the typical luminescence decay measured for a Si nanosphere. The lifetime derived from the exponential fitting of the luminescence decay was found to be ~ 30 ps, which is sufficiently short to virtualize the maximum blueshift of the MD resonance.

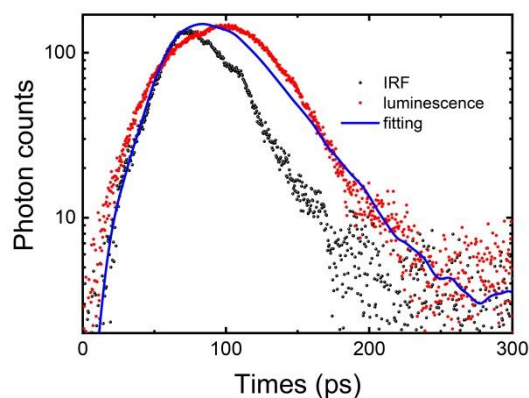


Figure S5: Luminescence decay measured for a Si nanosphere at ~ 580 nm. The instrument response function (IRF) and exponential fitting of the luminescence decay are also provided.

S6: Temperature rise in Si nanospheres induced by fs laser pulses

Owing to the heat accumulation effect, the temperature rise in a Si nanosphere induced by femtosecond laser pulses can be calculated by using the formula given in the following^[2-4].

$$\Delta T(r, t) = \sum_{n=1}^{num} \frac{Q}{8\rho c_p (\pi\alpha t)^{3/2}} \exp\left(-\frac{(r-r_0)^2}{4\alpha t}\right), \quad (2)$$

where $\rho = 1.1 \text{ kg m}^{-3}$, $c_p=1006.4 \text{ J kg}^{-1} \text{ K}^{-1}$ and $k=0.21 \text{ W m}^{-1} \text{ K}^{-1}$ are the density, specific heat and thermal conductivity of air and $\alpha = \frac{k}{\rho c_p}$. Here, $t = n*dt$ with n the pulse number and $dt = 13 \text{ ns}$ the inter-pulse time. For simplicity, the temperature distribution inside the Si nanosphere is assumed to be homogeneous and Si nanosphere is considered as a point heat source because its diameter ($d \sim 200 \text{ nm}$) is much smaller than that of the laser spot ($> 1.0 \mu\text{m}$). The absorption cross-section of the Si nanosphere can be calculated based on Mie theory:

$$\sigma_{sca} = \frac{2\pi}{k^2} \sum_{n=1}^{\infty} (2n+1) (|a_n|^2 + |b_n|^2), \quad (3)$$

$$\sigma_{ext} = \frac{2\pi}{k^2} \sum_{n=1}^{\infty} (2n+1) \text{Re}(a_n + b_n). \quad (4)$$

S7: Blue spectral shift, enhancement factor and quantum efficiency

In Fig. 4, we have presented the dependences of the blueshift of the MD resonance, the enhancement factor and quantum efficiency of the hot electron luminescence on the excitation intensity for a Si nanosphere which was resonantly excited at the EQ resonance. The reason why we chose the resonant excitation of the EQ resonance is the small blueshift of the EQ resonance, as compared with the MD and MQ resonances [see Fig. 1(c)], which enables the effective injection of electron-hole plasma into the Si nanosphere. In Fig. S6, we present the results obtained by resonantly exciting the MQ resonance of a Si nanosphere, which is known to possess the largest quality factor. In this case, it is noticed that the luminescence intensity is enhanced by one order of magnitude under the same excitation intensity as compared with the resonant excitation of the EQ resonance, as shown in Fig. S6(a). As a result, a larger quantum efficiency is obtained under the same excitation intensity and an increase of quantum efficiency with increasing excitation intensity is also observed, as can be seen in Figs. S6(c) and S6(d).

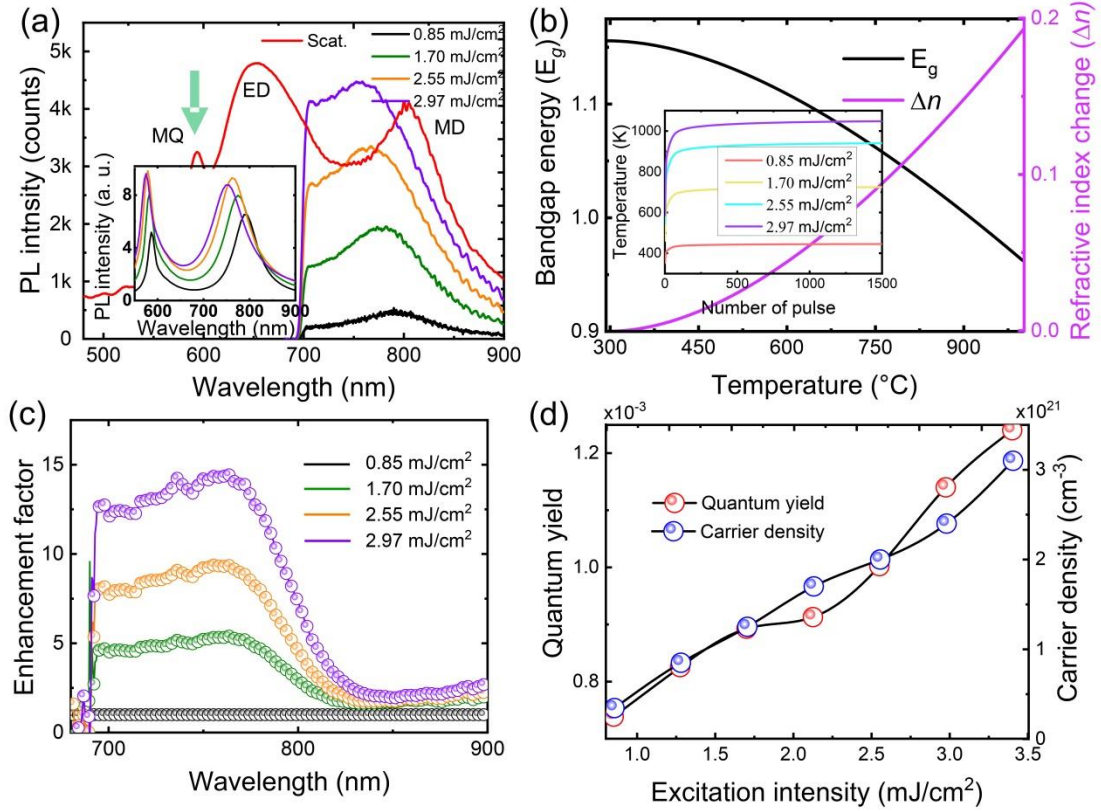


Figure S6: (a) Hot electron luminescence spectra measured for a Si nanosphere, which is excited at 590 nm, at different excitation intensities. The enhanced hot luminescence simulated for the Si nanosphere and the image of the hot electron luminescence are shown in the insets. (b) Dependence of the bandgap energy and refractive index change of Si on the temperature. The dependence of the temperature on the number of the irradiated pulse calculated for a Si nanosphere with $d \sim 200$ nm is shown in the inset. (c) Wavelength dependence of the enhancement factor for the hot electron luminescence calculated at different excitation intensities. (d) Dependence of the quantum yield and carrier density on the excitation intensity extracted for the Si nanosphere.

References

- [1] L. D. Landau, J. Bell, M. Kearsley, L. Pitaevskii, E. Lifshitz, and J. Sykes, *Electrodynamics of Continuous Media*, Vol. 8 (Elsevier Butterworth-Heinemann, Oxford, 1984).
- [2] P. Zijlstra, J.W.M. Chon, M. Gu, Effect of heat accumulation on the dynamic range of a gold nanorod doped polymer nanocomposite for optical laser writing and patterning, *Opt. Express*, 15,12151-12160 (2007).
- [3] Q. Dai, M. Ouyang, W. Yuan, J. Li, B. Guo, S. Lan, S. Liu, Q. Zhang, G. Lu, S. Tie, H. Deng, Y. Xu, M. Gu, Encoding Random Hot Spots of a Volume Gold Nanorod Assembly for Ultralow Energy Memory, *Adv. Mater.*, 29, 1701918 (2017).
- [4] G.P. Zograf, M.I. Petrov, D.A. Zuev, P.A. Dmitriev, V.A. Milichko, S.V. Makarov, P.A. Belov, Resonant Nonplasmonic Nanoparticles for Efficient Temperature Feedback Optical Heating, *Nano Lett.*, 17,2945-2952 (2017).